Heliyon 8 (2022) e12545

Contents lists available at ScienceDirect

Heliyon

journal homepage: www.cell.com/heliyon

Research article

A facile and high-sensitive bio-sensing of the V617F mutation in *JAK2* gene by GSH-CdTe-QDs FRET-based sensor

Fatemeh Hakimi [a], Maryam Khoshkam [b], Somayeh Sadighian [a,c], Ali Ramazani [c,d,*]

[a] Department of Pharmaceutical Biomaterials, School of Pharmacy, Zanjan University of Medical Sciences, Zanjan, Iran
[b] Chemistry Group, Faculty of Basic Sciences, University of Mohaghegh Ardabili, Ardabil, Iran
[c] Cancer Gene Therapy Research Center, Zanjan University of Medical Sciences, Zanjan, Iran
[d] Department of Pharmaceutical Biotechnology, School of Pharmacy, Zanjan University of Medical Sciences, Zanjan, Iran

ARTICLE INFO

Keywords:
Quantum dots
Biosensor
Janus kinase 2
V617F mutation
Fluorescence resonance energy transfer

ABSTRACT

This study aimed to directly detect the V617F point mutation of the Janus kinase 2 (*JAK2*) gene in the target DNA using a FRET-based biosensor. The water-soluble GSH-CdTe-QDs were synthesized by a one-step process, then GSH-QD conjugated to the termini amino-modified oligonucleotides target via carboxylic groups on the QD surface. The prepared QDs-DNA biosensor was applied in the quantitative and rapid detection of V617F mutation with a detection limit of 3×10^{-9} mol L^{-1} based on the FRET mechanism. In other words, detecting the V617F mutation by bio-sensing technology would be much simpler, cheaper, time-saving, highly sensitive, and more convenient than molecular diagnostic tools. Furthermore, the nano-biosensor was applied to detect the V617F mutation in clinical samples compared to the common ARMS-PCR (Amplification Refractory Mutation System-Polymerase Chain Reaction) standard method.

The results revealed that the GSH-capped biosensors would be effective for V617F mutation detection in samples distinguished with satisfactory analytical outcomes. Therefore, the designed fluorescence nanoprobe is suitable for the specific detection of V617F mutation of the *JAK2* gene in clinical samples.

1. Introduction

Myeloproliferative neoplasms (MPNs) are introduced as clonal disorders in the affected hematopoietic stem cell, leading to abnormal changes in peripheral blood and the generation of differentiated mature cells such as erythroid cells, megakaryocytes, and granulocytes [1, 2]. Multiple studies have demonstrated that somatic point mutations in the tyrosine kinase JAK2 protein are diagnosed in MPN disorders [3–5]. Single base mutation (G1849T) in the *JAK2* gene resulted in a valine to phenylalanine substitution at codon 617 (V617F) in the *JH2* pseudo-kinase domain [6–9]. The *JAK2* mutations and the abnormal changes in signal transduction can be caused hematopoietic and inflammatory disorders [10, 11]. In the last years, several molecular-based diagnostic techniques have been widely used for the detection of V617F mutation, including allele-specific PCR (AS-PCR), polymerase chain reaction with restriction fragment length polymorphism (PCR-RFLP), direct sequencing, high-resolution melting (HRM) analysis, and amplification refractory mutation system (ARMS) [8]. Thus far, despite the advantages of the techniques mentioned above, some drawbacks such as cost issues, complexity, selectivity and sensitivity, time-consuming, low DNA concentration of samples, proficiency, and contamination can be retained for clinical uses [12–14]. In the recent decade, bio-and nano-sensing technology have been promising ideas for addressing these limitations simultaneously due to its unique characteristics for identifying specific genes and mutations [13, 15]. Undoubtedly quantum dots (QDs) are an attractive kind of fluorescent nanomaterial in the field of bioassays owing to their optical properties in the Förster Resonance Energy Transfer (FRET) phenomenon [16, 17]. Ideally, compared with commonly used fluorescent dyes, QD-FRET probes with the QD as the donor have been provided a higher quantum yield (QY), higher sensitivity, fast response time, narrow emission spectra, long stability and lifetime, selective fluorescence signal, high surface density for immobilization of oligonucleotide, and the multicolor agents for biological diagnostic application [18–20]. The application of QDs FRET-based sensors in the biosensing of oligonucleotides was introduced by Zhang et al. for the first time to detect a point mutation in ovarian tumors [21]. Algar et al. designed another FRET system containing two different colors for the simultaneous detection of *SMN1* (Survival of Motor Neuron 1) and *LacZ* (gene for β-galactosidase of E. coli) genes in 2007 [22]. The target DNA

* Corresponding author.
E-mail address: ramazania@zums.ac.ir (A. Ramazani).

https://doi.org/10.1016/j.heliyon.2022.e12545
Received 2 July 2022; Received in revised form 7 November 2022; Accepted 14 December 2022

and single mismatch in hepatitis B virus (HBV) gene were detected by FRET reaction through CdSe/ZnS QDs-DNA bioconjugates [23]. Another report applied a QDs/DNA-AgNCs (silver nanoclusters) FRET-based probe to detect BRCA1 (Breast Cancer gene 1) gene deletion mutations with a detection limit of 1.2×10^{-13}M [24]. Besides, the detection of single-base mismatch mutations in the BRCA1 gene was detected via the FRET mechanism by CdTe-QDs and AgNCs [24]. Shamsipur et al. have designed a thiol-capped CdTe-QDs biosensor for rapid detection of human papillomavirus 18 (HPV18) DNA by FRET experiment with high sensitivity [25]. Moreover, a FRET experiment for a multicolor paper-based platform has been successfully applied to detect target DNA using green and red-emitting GSH-capped QDs with the limit of detection (LOD) in the range of femtomole [16]. Furthermore, other research has also been reported for the detection of oligonucleotide targets via FRET principle [26–30]. Till now, no sensor-based approach like GSH-CdTe-QDs probes has been reported for the detection of V617F mutation of *JAK2* gene. Here we introduced a CdTe-QDs biosensor for the detection of the V617Fmutation of *JAK2* gene. For this purpose, a FRET system was designed containing a CdTe-QDs probe modified with NH_2 as the donor and DNA labeled with Cy5 as the acceptor in the FRET pairs. The FRET phenomenon was done by forming the classic "sandwich" between QDs-DNA conjugates and complementary target DNA (Scheme 1). The designed nano-biosensor was employed for specific detection of single-base mutation in *JAK2* gene (V617F) through a fast and simple operational procedure without any excess washing and separation of the hybridized solution. Based on fluorescent intensity, the assay can be easily applied for low concentrations of target DNA. It is noticeable that successful functionalization of the CdTe-QDs surface and effective conjugating to the oligonucleotide was one of the advantages of this research. Such QDs-based biosensors can be suggested for sensitive and specific detection of *JAK2*mutation as a time-saving and inexpensive procedure in clinical investigations.

2. Materials and methods

2.1. Chemicals and reagents

Cadmium dichloride ($CdCl_2$), potassium telluride (K_2TeO_3), L-glutathione reduced (GSH≥98%), sodium citrate ($Na_3C_6H_5O_7.2H_2O$), sodium borate (Na_2 $[B_4O_5(OH)_4].8H_2O$,3-(3-dimethylaminopropyl), Tris-borate-ethylenediamine-tetra acetic-acid (TBE), 1-ethyl-3-(3-dimethylaminopropyl) carbodiimide (EDC), and N-hydroxysulfusuccinimide (NHS) and other chemicals were obtained from Sigma-Aldrich. All pre-solutions were prepared using ultra-pure water (18.3 MΩcm^{-1}). DNA Oligo products, including primers, probes, and templates, were designed based on the specific part of the JAK2 genome (GenBank accession number NG_009904.1) using the primer design program Primer3 [31] and PRIMER1 [32] and synthesized by Metabion international AG (Steinkirchen, Germany) as lyophilized powders as listed in Table 1. TheT4 DNA ligase kit was purchased from SinaClon Company (Tehran, Iran). *JAK2* positive clinical samples were obtained from the DeNA laboratory (Tehran, Iran (https://dna-lab.ir).

2.2. Synthesis and characterization of glutathione capped CdTe QDs

Water-soluble glutathione-capped CdTe quantum dots (GSH-CdTe-QDs) were successfully prepared according to the previously reported procedure with slight changes [33]. The green synthesis of GSH-CdTe-QDs was carried out under open-air atmospheric conditions using biocompatible compounds. In brief, a precursor solution of the $CdCl_2$ with a final concentration of 4mM was prepared in 50 mL of borate-citrate buffer (30mM in ultrapure water, pH 9). The mixture was stirred for 10 min at room temperature, and then GSH (10 mM) was added under high stirring as a reducing and capping agent. After 5 min, K_2TeO_3 (1 mM) was added, and the mixture was incubated at 90 °C. As a result, the GSH-CdTe-QDs were stabilized in red color after 120 min, and the reaction stopped at 4 °C. The GSH-CdTe-QDs were then purified from the water solution by adding 2 volumes of ethanol via centrifugation at 13000 ×g for 15 min, and finally, QDs dried for 24 h at room temperature. The prepared GSH-CdTe-QDs (1.84 μM) were stored at 4 °C in the

Table 1. Summary of the probe, primers, and DNA sequences used in this study.

Type	Abbreviations	Synthesis scale	Sequence 5'- 3'
DNA	CTDNA	0.04 μmol	TCTCGTCTCCACAGAAACATACTCCATAAT
DNA	MCTDNA	0.04 μmol	TCTCGTCTCCACAGAGACATACTCCATAAT
DNA	SDNA	0.2μmol	Cy5-ATTATGGAGTATGTT
DNA	PDNA	0.2 μmol	TCTGTGGAGACGAGATTTTTTTT-C_7Amino
DNA	FO	0.04 μmol	TCCTCAGAACGTGTATGGCAG
DNA	RO	0.04 μmol	ATT GCTTTCCTTTTTCACAAGAT
DNA	FWt	0.04 μmol	GCATTTGGTTTTAAATTATGGAGTATATG
DNA	RMt	0.04 μmol	GTTTTACTTACTCTCGTCTCCACA AAA

Complementary target DNA (CTDNA), Single base mismatch target DNA (MCTDNA), Probe DNA modified with NH_2 (PDNA), Single DNA labeled with Cy_5 (SDNA), Forward Oligo (FO), Reverse Oligo (RO), Forward Oligo Wild type (FWt), Reverse Oligo Mutant type (RMt).

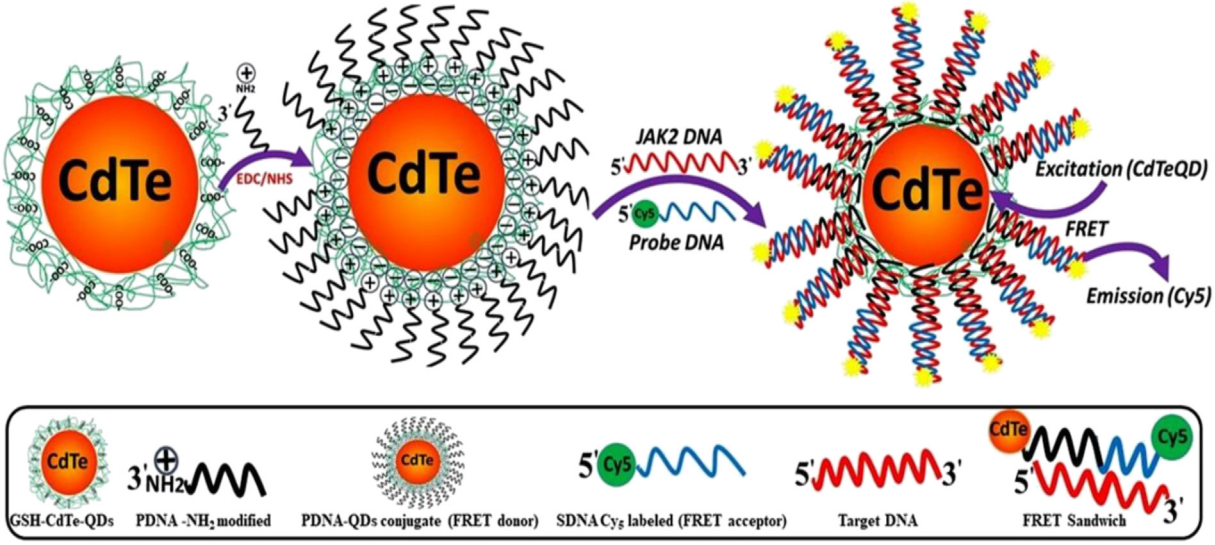

Scheme 1. The step by step synthesis process of developed biosensor.

dark (further details in the supplementary data). The obtained QDs were quite stable over several months without changing the spectroscopy properties (Figure S2). The High-resolution transmission electron microscopy (HRTEM FEI, TECNAI, F20 Philips) analysis was used to determine the morphology and particle size of GSH-CdTe-QDs. The Fourier transform infrared (FTIR) spectra of free GSH and GSH-CdTe-QDs were acquired by an FTIR instrument (FT-IR, TENSOR 27, BRUKER). The proton nuclear magnetic resonance (^{1}H NMR) spectroscopy (Ascend 850-BRUKER) confirmed the presence of glutathione on the surface of QDs. The optical responses (absorbance and fluorescence spectra) of prepared GSH-QDs were recorded by a UV transilluminator (MUV, CA, USA), Ultraviolet-Visible (UV-Vis) absorption Spectrophotometer (PG-T80+, UK), and an Infinite M-200-Pro microplate reader (Tecan, Austria, GmbH). The Zeta (ζ) potential measurements of GSH-CdTe-QDs were also done using a Brokhavan Zetasizer Nano (ZS) instrument.

2.3. Coupling and characterization of PDNA to GSH-CdTe-QDs

The functional carboxyl (COOH) groups at the surface of QDs provide colloidal stability and suitable sites for the covalent attachments to the amino-functionalized oligos [34, 35]. Self-assembly approaches can immobilize DNA strands on QDs surfaces [19]. For the preparation of PDNA-QDs conjugates, we designed a DNA sequence terminated with an amine (NH_2) group at the 3′ termini and conjugated to the QDs surface via the (EDC)/(NHS) standard strategy through amide bond formation [36]. Briefly, 40 μL of purified GSH−QDs (1.84 μM) were added to a glass vial and diluted with 20 μL of borate buffer (50 mM, pH 7.2), and an aqueous solution of EDC/NHS (10 μL, 50 mM) under a stir bar. The mixture was vortexed for 30 s. Subsequently, 20μL of PDNA (50 μM) was added to the above solution and then incubated under mild agitation for 1hour at 25 °C. The prepared PDNA-QDs conjugates were transferred to an Eppendorf microtube and centrifuged at 20000 rpm for 10 min. The supernatant was discarded, and the PDNA-QDs conjugates were suspended in borate buffer. PDNA-QDs solution was stored at 4 °C until future uses [17]. Gel electrophoresis assay and ζ-Potential measurements were performed on GSH-QDs and PDNA-QDs conjugates to confirm the conjugation of PDNA on the surface of QDs [22, 37]. Agarose gel (1%) prepared in TBE buffer (0.5X, pH 8.0). The electrophoresis was run at 80V for 40 min, and then the bands were visualized by UV transilluminator at 365nm.

2.4. Hybridization

Detection of CTDNA was carried out by hybridization reaction in a constant volume of buffer solution containing Tris–HCl 10 mM, NaCl 0.1 M, $MgCl_2$ 5 mM, EDTA10 mM, pH 8.0. In brief, 80 μL of PDNA-QDs conjugates, 10 μL of SDNA (10 μM) and the calculated amounts of CTDNA/PDNA-QDs (R) (R = 200, 100, 50, 20, 10, 5, 2, 0.5, 0) with equal concentrations (1.5, 0.75, 0.3, 0.15, 0.075, 0.03, 0.012, 0.003, and 0 μM in final solution, respectively) were mixed in Tris buffer solution. In this experiment, the amount of PDNA-QDs conjugate and SDNA were kept constant, and only the amount of the CTDNA was changed, whereas the total volume of reaction was constant (200 μL). The reaction was allowed to keep at 37 °C for 1 hr and then cooled to 4 °C. The fluorescent measurements were also carried out at λ_{ex}: 420 nm. Tris buffer was used as a blank.

2.5. Fluorescence detection of a single base mutation in JAK2 gene

A detection experiment of single base mismatch mutation was performed in a T4 ligation buffer. To accomplish the reaction, 140μL of PDNA-QDs conjugate with 20μL of SDNA (10 μM), 20 μL of MCTDNA (10 μM), were added to 30 U of T4 DNA ligase, and 20 μL of T4 ligation buffer (230 μL total volume). Finally, the mixture was incubated at 37 °C for 1 hr. After cooling, the fluorescence measurements were taken on an Infinite M-200-Pro microplate reader instrument (Tecan, Austria, GmbH).

2.6. Mutation detection by ARMS-PCR assay as a standard protocol

Genomic DNA was extracted from peripheral blood samples using the salting-out method [38]. Next, the concentration of the DNA samples was measured by the NanoDrop 2000/2000c spectrophotometer (Thermo Scientific, USA) and stored at -20 °C for further analysis. PCR reaction consisted of 12.5 μL 2x PCR master mixes (Fermentas, USA), 200 ng of DNA template, 50 nM of each primer (RO, Fwt, FO, and RMt), and nuclease-free water up to 25 μL.

The ARMS-PCR assay was performed, as the gold standard method for detection of the V617F point mutation in clinical samples, by a Thermal Cycler (iCycler, Bio-Rad, USA) instrument under the following program; initial denaturation cycle at 95 °C for 5 min, 40 cycles of template denaturation at 95 °C for the 30 s, annealing at 59 °C for 30s, extension at 72 °C for 30 s, and, final extension holds at 72 °C for 7 min [39]. The mutant and non-mutant DNA templates were used as a positive and negative control, respectively. Then, the PCR amplicons were characterized by gel electrophoresis in 2% agarose gel in TBE buffer (0.5x, pH 8.0). The gel electrophoresis was run at 100 V for 45 min, and the samples were visualized by a UV transilluminator. This study was approved by institutional ethical committee of Zanjan University of Medical Sciences (Ethical code: IR. ZUMS.REC.1398.459).

3. Results and discussion

3.1. Synthesis and physical characterization of QDs

The choice of a donor molecule with colloidal stability and high quantum yields is also notable for the success of the FRET mechanism. Indeed, some literatures reported that the best fluorescence yields are attributed to larger QDs [40–42]. In this regard, red GSH-CdTe-QDs were

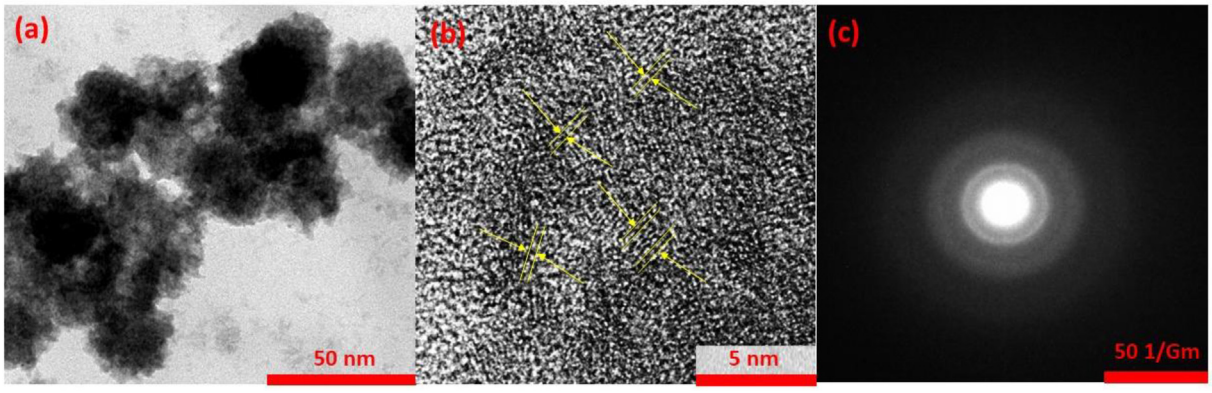

Figure 1. (a) Low resolution and (b) High resolution TEM images and (c) SAED pattern for GSH-CdTe-QDs.

synthesized after 120 min and optimized for this study (further details in Figure S2 of supplementary data). Furthermore, the structural and optical characterizations of the prepared GSH-CdTe-QDs were analyzed by the HR-TEM, FT-IR, ^{1}HNMR, UV-Vis, and Fluorescence (FL) spectroscopy. Indeed, the size and morphology of GSH-CdTe-QDs as a tiny core nanocrystal can be exactly evaluated by the HR-TEM microscopy technique [43]. As shown in HR-TEM and SAED pattern micrographs (Figure 1) the synthesized GSH-CdTe-QDs exhibit cubic crystalline structure. CdTe displays a cubic crystalline structure that allows it to function as a semiconductor. The size of the QDs varies between 3-4 nm in ultrapure-water pH 7.4. Besides, the insertion of CdTe-QDs nanocrystals in the GSH layers can increase the stability of the synthesized QDs.

Further, FT-IR and ^{1}HNMR techniques have been used for the surface binding characterization of the QDs [44]. For further confirmation, the NMR experiment was applied for ligands attached to distinguish the GSH in a free state and bound to the CdTe-QDs surface [45]. The FT-IR and NMR studies revealed that the GSH ligands had been successfully conjugated onto the CdTe-QDs surface through Cd–S covalent interactions (further details in Figure S3 at supplementary data).

3.2. PDNA-QDs conjugate characterization

Electrophoretic mobility shift assay and ζ-Potential measurements were convenient methods to characterize the QDs before and after conjugation. As previously reported, the electrophoretic velocity of the bio-conjugate materials resulted in charge-to-mass ratio changes, which can be verified by gel electrophoresis [46, 47]. Mobility shift assay can prove the successful attachment of PDNA onto the surface of GSH-CdTe-QDs. The results of gel electrophoresis analysis using 1% w/v agarose in 0.5x TBE buffer of GSH-CdTe-QDs and PDNA-QDs conjugates have been indicated in Figure 2. In lane 1, GSH-CdTe-QDs and in lane 2, PDNA-QDs conjugates were loaded. As shown in Figure 2, PDNA-QDs conjugates immigrated faster than GSH-CdTe-QDs, which is caused by the conjugating of the PDNA to the GSH-CdTe-QDs surfaces increasing its negative charge. Besides, electrophoretic behavior changes can be attributed to the conformation of PDNA-QDs conjugates the ζ-Potential changes further confirmed the attachment of PDNA to QDs. PDNA presence at the surface of QDs after the coupling increases its negative charge. The ζ-Potential values were obtained -35 and -80 mV for GSH-CdTe-QDs and PDNA-QDs, respectively, which fully confirms the coupling of the positively charged NH_2-modified PDNA to the negatively charged GSH-CdTe-QDs. Significantly, the conjugation efficiency of the (EDC)/(NHS) standard procedure used in this study depends on pH value. The optimized pH for the typically used EDC/NHS mediated reactions has been investigated at 6–8. At very acidic or alkaline conditions, the fluorescence responses of thiol-capped QDs bioconjugates can be decreased and become unstable. For example, the coupling yield and the number of captured DNA on each QD significantly decreased at pH 8.0 and 6.0, respectively. Therefore, the pH of 7.2 around physiological pH was utilized to balanced efficiency and stability in the conjugation reaction [24, 48].

3.3. Optical characterization

Totally, the spectral properties of the fluorescence pair affect FRET efficiency for the bio-sensing process. Figure 3 represents the absorbance and emission spectra properties of GSH-CdTe-QDs, PDNA-QDs, and Cy5 as a designed FRET-based system. To determine the best excitation wavelength and minimize the inner filter effects, the experiments were done at λ_{ex} attributed to concentrations of CdTe-QDs that absorbance density is < 0.1. In this regard, the λ_{ex} can be set according to the longest wavelength absorption band at the red edge of fluorescent spectra. Therefore the excitation wavelength was chosen at 420 nm as λ_{ex} for further experiments [49]. As shown in Figure 3, the broad absorption band of the GSH-CdTe-QDs allows flexibility in choosing a suitable excitation wavelength to excite the QDs with minimum interference from

Figure 2. Agarose gelelectrophoresis (1%) in TBE buffer 0.5x of the GSH-CdTe-QDs (lane 1) and PDNA-QDs conjugate (lane 2).

background emission. Due to the significant spectral overlap as a requirement of FRET between the PDNA-QDs and Cy5, the FRET phenomenon can be accrued between QDs and Cy5 as donor-acceptor pairs. Additionally, according to Figure 3, it is observed that the coupling of PDNA did not interfere with the absorption and emission spectra GSH-CdTe-QDs. As a result, the size of QDs upon conjugation was nearly mono-disperse and homogeneous as GSH-CdTe-QDs with no change in their optical properties. The fluorescence spectrum of GSH-CdTe-QDs

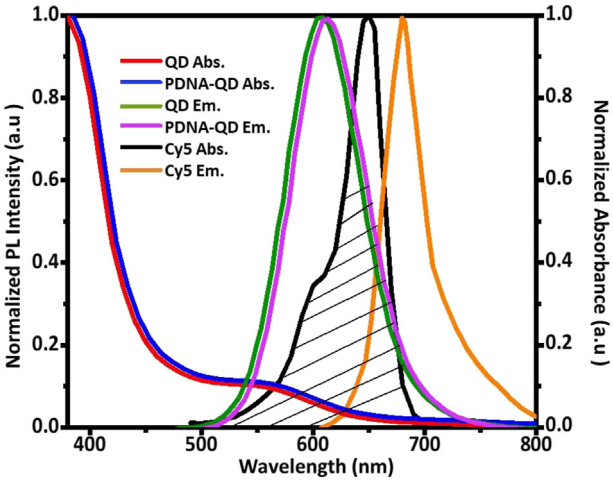

Figure 3. Normalized UV−vis absorption spectra and FL spectra of the pure GSH-CdTe-QDs, PDNA-QDs conjugate and Cy5 at λ_{em}: 420nm.

and PDNA-ODs were shown very narrow emission bandwidths with similar FWHM (full width half maximum) of about 40nm. The result suggests that the GSH-CdTe-QDs and Cy5 were ideal fluorophores as a FRET pairs that permitted FRET occurrence exactly. To evaluate the FRET efficiency of this fluorescent probe, the quantum yield (Φ) of the prepared QDs was estimated at 20% (using the fluorescein as a standard fluorophore), in agreement with the other thiol-capped QDs as reported in the literature.

Fluorescence quantum yields of QDs calculated using a relative method. The fluorescence quantum yield of fluorescein was obtained at 90% (in 0.1 M NaOH solution) of the literature. [Φ] for the synthesized QDs was determined according to the following equation:

$$\varnothing = \varnothing_{standard} \frac{n^2}{n_{st}^2} \left(\frac{A}{A_{St}} \right)$$

Where Φ was the quantum yield, n was the refractive index of solvent (1.33 for water and 1.335 for NaOH), and A is the slope of the plot of integrated fluorescence intensity *vs.* absorbance [41, 50–52] (further details in Figure 4).

Förster distance (R_0), the distance of the donor-acceptor pair at 50% FRET efficiency typically in the range of 2–10 nm, in our FRET system obtained~7 nm, according to previous studies. The FRET parameter was calculated using the analytical-based software [53, 54] (further details in the supplementary data).

3.4. FRET detection

The FRET-based experiment was done to detect V617F mutation in the *JAK2* gene. To evaluate the sensing capability of nanoprobe for detecting the CTDNA, we assembled the PDNA-QDs conjugation in the presence of CTDNA and SDNA. They formed a PDNA-QD/SDNA/CTDNA complex through the hybridization reaction. The hybridization reaction was accomplished by mixing the varying ratios from CTDNA to PDNA-QD (R) in Tris buffer as solvent. When the sandwich complexes exited at λ_{ex}: 420 nm, the spectral overlap, and cross-talk between PDNA-QDs and SDNA lead to energy transfer to the Cy5 dye, resulting in a FRET signal that can be utilized to recognize CTDNA with high efficiency. In order to evaluate the concentration effect on the FRET response, a range of concentrations containing 1.5, 0.75, 0.3, 0.15, 0.075, 0.03, 0.012 and 0.003 μM of CTDNA was examined.

After adding CTDNA into the hybridization solution, it formed a sandwich structure with PDNA-QDs and SDNA. When several sandwich hybrids are successfully formed in each local concentration of targets, signal QDs enriched in a nanoscale domain. Due to hybridization interaction in the CTDNA, SDNA and PDNA-QDs are placed at a satisfying distance of the Förster radius (R_0), resulting in the transfer of energy via the FRET phenomenon. In this manner, the indirect excitation of Cy5 at the excitation wavelength of the QDs allowed CTDNA qualitatively to distinguish with a very low background signal. Figure 4a shows the fluorescence spectra of Cy5, Tris buffer (as a blank solution), nano-sandwiched hybrid, and non-hybrid systems. The direct excitation of Cy5 at the excitation wavelength of QD was investigated as variable control in this experiment. As indicated in Figure 4a, tris buffer and Cy5 alone have no significant emission when they exited at the excitation wavelength of GSH-CdTe-QDs. In the absence of CTDNA (R = 0, as a negative control), the pairing does not occur, and therefore, fluorescence is only emitted from PDNA-QDs. Figure 4a clearly indicated that all the hybrid nano-sandwiches containing the different concentrations of CTDNA showed a stoke shift at the emission maximum position compared to the negative control (R = 0, containing PDNA-QDs and SDNA with constant concentrations). Generally, the stoke shift to the higher wavelength (redshift) is related to the size increase of QDs [40, 42].

Furthermore, with the increase of the CTDNA fragments, the hydrodynamic radius of QDs samples increased due to the aggregation of sandwich structures. Therefore, as the number of hybrid nano-sandwiched increased on the QDs surface, fluorescence emission spectra of the samples shifted to longer wavelengths due to the size increase of hybrid molecules. In addition, as observed, the FRET efficiency promotes by an increasing number of hybrid molecules and a redshift in the emission maximum of hybrid molecules at the wavelength close to λ_{ex} of the Cy5. These relative changes in the system's fluorescence intensity can result in the FRET phenomenon occurrence.

To examine the selectivity of the nanoprobe, a hybridization reaction was carried out to distinguish the MCTDNA from the CTDNA. As shown in Figure 4b, the fluorescence emission spectrum of the PDNA-QDs has no prominent change in the presence of the MCTDNA (at a ratio of R = 100) compared to the fluorescence emission spectrum of the PDNA-QDs. Besides, this result reveals that the FRET reaction did not occur between PDNA-QDs and SDNA in the presence of MCTDNA. Furthermore, suggesting that MCTDNA fragments could be sensitively and selectively distinguished by QDs bio-probe as well as CTDNA.

The limit of detection (LOD) of the nano-sandwiched system was calculated to be 3×10^{-9} mol L^{-1} using the Stern−Volmer equation ($F_0/F = 1 + K_{sv}$ [Q]), where F_0/F is the intensity fluorescence of PDNA-QDs nanoprobe. In this equation, the fluorescence intensity of PDNA-QDs nanoprobe in the absence and presence of SDNA probe and complementary DNA are signed by F_0 and F, respectively, the [Q] is the CTDNA concentration, and K_{sv} constant is signed as the fluorescence lifetime or quenching coefficient of the system (as the slope of the Stern-Volmer curve) [26, 55, 56].

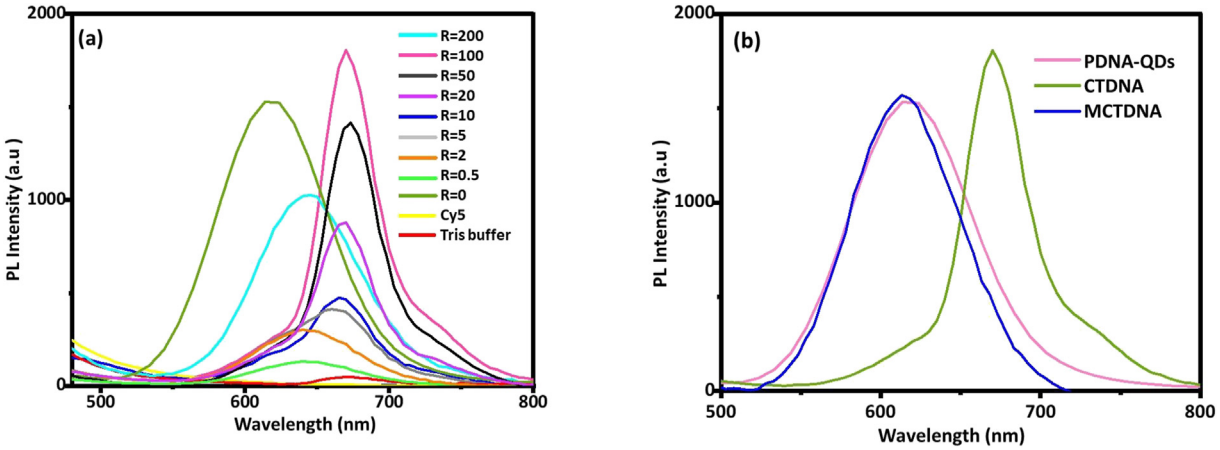

Figure 4. (a) FL spectra of nano-biosensor containing various concentrations of complementary DNA (R) in Tris buffer and at λ_{em}: 420nm; (b) FL spectra of the PDNA-QDs, MCTDNA and CTDNA target (R = 100) in Tris buffer and at λ_{em}: 420nm.

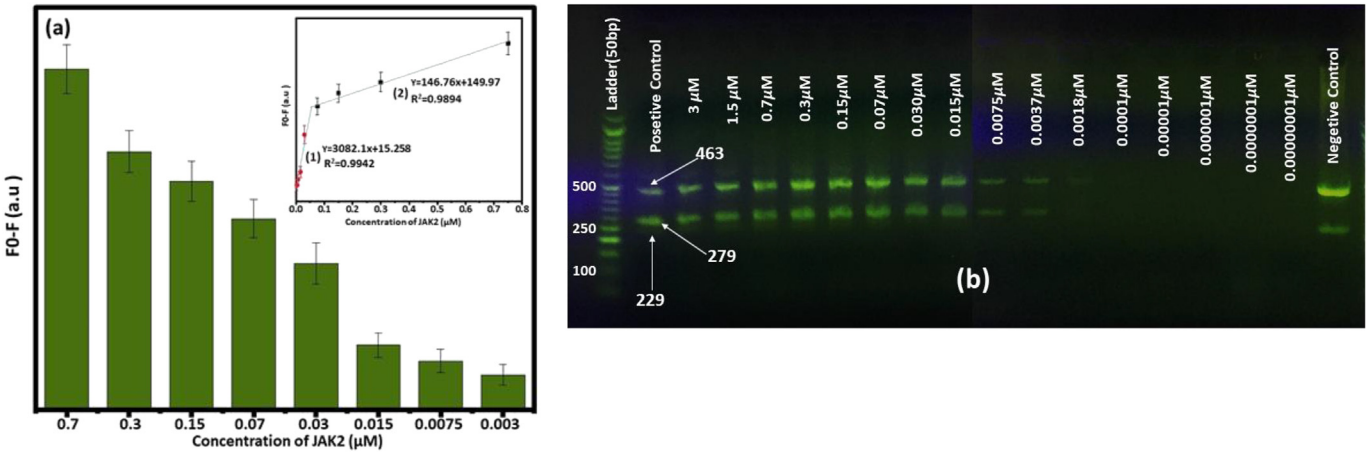

Figure 5. (a) Fluorescence responses of a hybrid system containing different concentrations of V617F samples were recorded at λ_{em}: 420nm, that F_0 and F are attributed to the fluorescence intensities of PDNA-QDs in the absence and presence of SDNA-probe and V617F DNA samples, respectively. (b) Representative agarose gel electrophoresis (2%) of ARMS-PCR assays for different concentrations of V617F DNA samples under light UV (362nm).

Herein, the Stern−Volmer equation was obtained as Y = 15.487 X + 1.0696 at five concentrations levels of 0.075, 0.03, 0.016, 0.012 and 0.007μM with a regression (r) of 0.9848.

3.5. Detection of V617F mutation in clinical samples by biosensor

To validate the practicality and feasibility of the designed fluorescent probe in the clinical samples, the nanoprobe system was examined for V617F mutation detection in the clinical setting. So, the different concentrations (0.7, 0.3, 0.15, 0.07, 0.03, 0.015, 0.0075, and 0.003 μM in final solution) equal with R (100, 50, 20, 10, 5, 2, 1 and 0.5, respectively) of V617F positive samples were tested based on a hybrid system by biosensor. It should be noted that this experiment was done under the conditions mentioned above for a CTDNA. Also, to evaluate the accuracy of the biosensor, ARMS-PCR was performed for the qualitative detection of mutation in clinical samples (ranges of 3, … and 0.01 $\times$ $10^{-12}\mu$M) compared to the biosensor assay. In these experiments, DNA samples from the healthy volunteerswere tested (DNA without mutation, R = 100) as a negative control. The fluorescence intensity or FRET signal as the response function (F_0–F) of the biosensor was evaluated for different concentrations of V617F positive samples as target molecules at λ_{em}:420 nm Figure 5 indicated the plot of (F_0–F) (a) and gel electrophoresis image (b) containing different concentrations of V617F positive samples. Here, a linear relationship exist between the fluorescence response function and V617Fmutationat both low and high concentrations. The linearity with regression of 0.9942 and 0.9894 were obtained for the detection of V617Fmutationin this study. In addition, the FRET signal can gradually be saturated in the higher concentration of target DNA which was assigned to the depletion of the active hybridization sites onto the QDs surface. Too, due to the depletion of the available sites, the linearity behavior in the higher concentration can differ compared to the lower concentrations. As indicated in Figure 5a, the planned biosensor showed good selectivity for V617F mutation detection in the clinical samples. The response function of a hybrid system containing the target DNA decreased with decreasing concentration. In addition, if the concentration is higher, the response function is also more, resulting in much energy transferring from PDNA-QDs to the SDNA probe at a higher concentration. Additionally, there are no sandwiched hybrids and FRET reactions in the negative real sample. As a result, the fluorescence intensity [F] there is no change compared to [F_0] (fluorescence intensity of PDNA-Qds). Thus, the response function of the biosensor [F] is the same F_0 (F_0–F = 0). This result suggested that the biosensor clearly and selectively distinguishes between positive and negative samples. As shown in Figure 5b, the FO and RO common primers produced an amplicon size of 463 bp from the *JAK2* gene. Indeed, the 229 and 279 pb bands attributed to wild-type and mutant allele, respectively, indicating the presence of the V617F mutation as a heterozygote. As can be seen from Figure 5b, the bands of the amplification products *JAK2* DNA were obvious for the concentration's ranges of 3–0.0037 μM; the bands related to 0.0075 and 0.0037 μM concentrations are very weak. As shown in Figure 5b, there is noPCR band in values of 0.0018, ….,0.01 $\times$ 10^{-12} μM for the amplification products. As a result, the outcomes of the fluorescence assay had good agreement with the results of the ARMS-PCR method.

4. Conclusion

Herein, a versatile and simple diagnostic tool was designed for the detection of theV617F mutation in the *JAK2* gene. We prepared a fluorescent biosensor based on carboxyl-functionalized-CdTe-QDs attached with amino-modified DNA. Fabrication and application of QDs-based biosensors are simple and efficient for diagnostic approaches. The biosensor for the sensitive detection and selective hybridization of target DNA was examined based on the FRET signals. The "nano-sandwiched" hybrid structures composed of the QD-dye pair and CTDNA are formed that promote the fluorescence intensity of Cy5 acceptor by transferring energy in the donor-acceptor complex through the FRET mechanism. In addition, the maximum emission wavelength for the bioprobe showed a significant redshift near the emission maximum of Cy5. We found that the further redshift and increasing fluorescence intensity at a higher concentration of target molecules occur simultaneously. Herein, the number of sandwiched hybrid structures has been increased with a more effective and higher yield for the FRET reaction. FTIR, HR-TEM, and ^{1}H NMR analyses characterized the GSH-CdTe QDs. Zeta potential and fluorescence measurements were done before and after conjugation. Furthermore, the prepared nano-biosensor could also successfully discriminate and detect the V617F positive clinical DNA samples, indicating that the nano-biosensing can be valuable for performing quantitative analysis in biological diagnosis and clinical practice.

Declarations

Author contribution statement

Fatemeh Hakimi: Performed the experiments; Analyzed and interpreted the data; Wrote the paper.

Maryam Khoshkam; Somayeh Sadighian: Analyzed and interpreted the data; Contributed reagents, materials, analysis tools or data.

Ali Ramazani: Conceived and designed the experiments; Analyzed and interpreted the data.

Funding statement

Prof. Ali Ramazani was supported by Zanjan University of Medical Sciences [A-12-349-38].

Data availability statement

Data included in article/supp. material/referenced in article.

Declaration of interest's statement

The authors declare no competing interests.

Additional information

Supplementary content related to this article has been published online at 10.1016/j.heliyon.2022.e12545.

References

[1] M. Mejía-Ochoa, P.A. Acevedo Toro, J.A. Cardona-Arias, Systematization of analytical studies of polycythemia vera, essential thrombocythemia and primary myelofibrosis, and a meta-analysis of the frequency of JAK2, CALR and MPL mutations: 2000-2018, BMC Cancer 19 (2019) 590.

[2] M. Maddali, U.P. Kulkarni, N. Ravindra, E. Jajodia, A.K. Arunachalam, H. Suresh, A. Venkatraman, B. George, V. Mathews, P. Balasubramanian, JAK2 exon 12 mutations in cases with JAK2V617F-negative polycythemia vera and primary myelofibrosis, Ann. Hematol. 99 (2020) 983–989.

[3] S. Demyanets, E. Jaeger, E. Pablik, G. Greiner, S. Herndlhofer, P. Valent, I. Schwarzinger, The JAK2 blocker TG101209 is a potent inhibitor of clonogenic progenitor cell growth in patients with chronic myeloid leukaemia, Br. J. Haematol. 181 (2018) 137–139.

[4] J. Grinfeld, J. Nangalia, E.J. Baxter, D.C. Wedge, N. Angelopoulos, R. Cantrill, A.L. Godfrey, E. Papaemmanuil, G. Gundem, C. MacLean, J. Cook, L. O'Neil, S. O'Meara, J.W. Teague, A.P. Butler, C.E. Massie, N. Williams, F.L. Nice, C.L. Andersen, H.C. Hasselbalch, P. Guglielmelli, M.F. McMullin, A.M. Vannucchi, C.N. Harrison, M. Gerstung, A.R. Green, P.J. Campbell, Classification and personalized prognosis in myeloproliferative neoplasms, N. Engl. J. Med. 379 (2018) 1416–1430.

[5] J.J. Kiladjian, The spectrum of JAK2-positive myeloproliferative neoplasms, Hematology Am. Soc. Hematol. Educ . Program (2012) 561–566, 2012.

[6] H. Asadzadeh-Aghdaei, K. Mashayekhi, K. Koushki, P. Azimzadeh, M. Rostami-Nejad, D. Amani, V. Chaleshi, S.M. Haftcheshmeh, A. Sahebkar, M.R. Zali, V617F-independent upregulation of JAK2 gene expression in patients with inflammatory bowel disease, J. Cell. Biochem. 120 (2019) 15746–15755.

[7] A.J. Bench, E.J. Baxter, A.R. Green, Methods for detecting mutations in the human JAK2 gene, Methods Mol. Biol. 967 (2013) 115–131.

[8] A. Keller, B. Wingelhofer, B. Peter, K. Bauer, D. Berger, S. Gamperl, M. Reifinger, S. Cerny-Reiterer, R. Moriggl, M. Willmann, P. Valent, E. Hadzijusufovic, The JAK2/STAT5 signaling pathway as a potential therapeutic target in canine mastocytoma, Vet. Comp. Oncol. 16 (2018) 55–68.

[9] Y.L. Zhao, G.M. Liu, L.J. Zhang, W.T. Liang, Z.Y. Cheng, [Inhibitors of JAK2/STAT signaling pathway and hematologic malignancies-review], Zhongguo Shi Yan Xue Ye Xue Za Zhi 24 (2016) 1275–1279.

[10] F.M. Mohammed, H. Pakzad, V.R. Esfahani, Evaluation of V617F JAK 2 gene mutation by high resolution Melting method in patient with erythrocytosis, J. Personalized Med. 5 (2020) 9–11.

[11] K.L.P. Tun, A.Z. Latt, W.P.P. Naing, S. San Htwe, Y.K. Ko, W.W. Mar, W.W. Han, S. Win, Identification of JAK2 (V617F) mutation in myeloproliferative neoplasms by using allele specific polymerase chain reaction (AS-PCR), Am. J. Mol. Biol. 10 (2020) 273.

[12] A.J. Bench, H.E. White, L. Foroni, A.L. Godfrey, G. Gerrard, S. Akiki, A. Awan, I. Carter, A. Goday-Fernandez, S.E. Langabeer, T. Clench, J. Clark, P.A. Evans, D. Grimwade, A. Schuh, M.F. McMullin, A.R. Green, C.N. Harrison, N.C. Cross, Molecular diagnosis of the myeloproliferative neoplasms: UK guidelines for the detection of JAK2 V617F and other relevant mutations, Br. J. Haematol. 160 (2013) 25–34.

[13] P.-I. Gouma, Nanomaterials for Chemical Sensors and Biotechnology, Pan Stanford Publishing, 2010.

[14] G. Maduraiveeran, M. Sasidharan, V.J.B. Ganesan, Bioelectronics, Electrochemical sensor and biosensor platforms based on advanced nanomaterials for biological and biomedical applications, Biosens. Bioelectron. 103 (2018) 113–129.

[15] N. Hildebrandt, C.M. Spillmann, W.R. Algar, T. Pons, M.H. Stewart, E. Oh, K. Susumu, S.A. Díaz, J.B. Delehanty, I.L. Medintz, Energy transfer with semiconductor quantum dot bioconjugates: a versatile platform for biosensing, energy harvesting, and other developing applications, Chem. Rev. 117 (2017) 536–711.

[16] M.O. Noor, U.J. Krull, Paper-based solid-phase multiplexed nucleic acid hybridization assay with tunable dynamic range using immobilized quantum dots as donors in fluorescence resonance energy transfer, Anal. Chem. 85 (2013) 7502–7511.

[17] D. Sun, O. Gang, DNA-functionalized quantum dots: fabrication, structural, and physicochemical properties, Langmuir: the ACS journal of surfaces and colloids 29 (2013) 7038–7046.

[18] C.T. Matea, T. Mocan, F. Tabaran, T. Pop, O. Mosteanu, C. Puia, C. Iancu, L. Mocan, Quantum dots in imaging, drug delivery and sensor applications, Int. J. Nanomed. 12 (2017) 5421–5431.

[19] A. Sedighi, U.J. Krull, Rapid immobilization of oligonucleotides at high density on semiconductor quantum dots and gold nanoparticles, Langmuir: the ACS journal of surfaces and colloids 32 (2016) 13500–13509.

[20] C.Y. Zhang, H.C. Yeh, M.T. Kuroki, T.H. Wang, Single-quantum-dot-based DNA nanosensor, Nat. Mater. 4 (2005) 826–831.

[21] W.R. Algar, U.J. Krull, Towards multi-colour strategies for the detection of oligonucleotide hybridization using quantum dots as energy donors in fluorescence resonance energy transfer (FRET), Anal. Chim. Acta 581 (2007) 193–201.

[22] X. Wang, X. Lou, Y. Wang, Q. Guo, Z. Fang, X. Zhong, H. Mao, Q. Jin, L. Wu, H. Zhao, J. Zhao, QDs-DNA nanosensor for the detection of hepatitis B virus DNA and the single-base mutants, Biosens. Bioelectron. 25 (2010) 1934–1940.

[23] Y.S. Borghei, M. Hosseini, M.R. Ganjali, S. Hosseinkhani, A novel BRCA1 gene deletion detection in human breast carcinoma MCF-7 cells through FRET between quantum dots and silver nanoclusters, J. Pharmaceut. Biomed. Anal. 152 (2018) 81–88.

[24] Y.S. Borghei, M. Hosseini, M.R. Ganjali, H. Ju, A unique FRET approach toward detection of single-base mismatch DNA in BRCA1 gene, Materials science & engineering, C, Materials for biological applications 97 (2019) 406–411.

[25] M. Shamsipur, V. Nasirian, K. Mansouri, A. Barati, A. Veisi-Raygani, S. Kashanian, A highly sensitive quantum dots-DNA nanobiosensor based on fluorescence resonance energy transfer for rapid detection of nanomolar amounts of human papillomavirus 18, J. Pharmaceut. Biomed. Anal. 136 (2017) 140–147.

[26] G.R. Bardajee, M. Zamani, M. Sharifi, Efficient and versatile application of fluorescence DNA-conjugated CdTe quantum dots nanoprobe for detection of a specific target DNA of SARS Cov-2 virus, Langmuir : the ACS journal of surfaces and colloids 37 (2021) 10223–10232.

[27] M. Dekaliuk, X. Qiu, F. Troalen, P. Busson, N. Hildebrandt, Discrimination of the V600E mutation in BRAF by rolling circle amplification and förster resonance energy transfer, ACS Sens. 4 (2019) 2786–2793.

[28] A.A. Ensafi, N. Kazemifard, B. Rezaei, A simple and rapid label-free fluorimetric biosensor for protamine detection based on glutathione-capped CdTe quantum dots aggregation, Biosens. Bioelectron. 71 (2015) 243–248.

[29] M. Mazloum-Ardakani, R. Aghaei, M.M. Heidari, Quantum-dot biosensor for hybridization and detection of R3500Q mutation of apolipoprotein B-100 gene, Biosens. Bioelectron. 72 (2015) 362–369.

[30] A. Shahmuradyan, M. Moazami-Goudarzi, F. Kitazume, G.S. Espie, U.J. Krull, Paper-based platform for detection by hybridization using intrinsically labeled fluorescent oligonucleotide probes on quantum dots, Analyst 144 (2019) 1223–1229.

[31] T. Koressaar, M. Remm, Enhancements and modifications of primer design program Primer3, Bioinformatics 23 (2007) 1289–1291.

[32] A. Collins, Primer1: primer design web service for tetra-primer ARMS-PCR, Open Bioinf. J. 6 (2012) 55–58.

[33] J.M.P. Donoso, J.P.M. Charles, I.O. Osorio-Roman, C.C.V. Guzman, Synthesis of Highly Fluorescent GSH-CDTE Nanoparticles (Quantum Dots), Google Patents, 2017.

[34] A. Banerjee, T. Pons, N. Lequeux, B. Dubertret, Quantum dots-DNA bioconjugates: synthesis to applications, Interface focus 6 (2016), 20160064.

[35] Y. Han, M.O. Noor, A. Sedighi, U. Uddayasankar, S. Doughan, U.J. Krull, Inorganic nanoparticles as donors in resonance energy transfer for solid-phase bioassays and biosensors, Langmuir : the ACS journal of surfaces and colloids 33 (2017) 12839–12858.

[36] A. Samanta, Z. Deng, Y. Liu, H. Yan, A perspective on functionalizing colloidal quantum dots with DNA, Nano Res. 6 (2013) 853–870.

[37] D.N. Williams, J.S. Saar, V. Bleicher, S. Rau, K. Lienkamp, Z. Rosenzweig, Poly(oxanorbornene)-Coated CdTe quantum dots as antibacterial agents, ACS Appl. Bio Mater. 3 (2020) 1097–1104.

[38] Z. Ghasemi, M. Hashemi, M. Ejabati, S.M. Ebrahimi, H. Kheiri Manjili, A. Sharafi, A. Ramazani, Development of a high-resolution melting analysis method for CYP2C19*17 genotyping in healthy volunteers, Avicenna J. Med. Biotechnol. (AJMB) 8 (2016) 193–199.

[39] P. Karimzadeh, S.H. Ghaffari, S. Ferdowsi, B. Chahardouli, Z. Saltanatpouri, N. Einollahi, S.A. Mousavi, B. Bahar, H. Dargahi, G. Togheh, Comparisons of ARMS-PCR and AS-PCR for the evaluation of JAK2V617F mutation in patients with non-CML myeloproliferative neoplasms, Int. J. Hematol. Oncol. Stem Cell Res. (2010) 10–13.

[40] O.S. Oluwafemi, J. Flowers, O.O. Adeyemi, S. Bhagyaraj, V. Ncapayi, N. Zikalala, E.T. Gwebu, One pot synthesis of stable water soluble thiol capped CdTe nanoparticles: effect of precursor ratio, refluxing time and capping group on the optical property, Nano-Structures & Nano-Objects 17 (2019) 223–228.

[41] J.M. Pérez-Donoso, J.P. Monrás, D. Bravo, A. Aguirre, A.F. Quest, I.O. Osorio-Román, R.F. Aroca, T.G. Chasteen, C.C. Vásquez, Biomimetic, mild chemical synthesis of CdTe-GSH quantum dots with improved biocompatibility, PLoS One 7 (2012) e30741, e30741.

[42] J.C.L. Sousa, M.G. Vivas, J.L. Ferrari, C.R. Mendonca, M.A. Schiavon, Determination of particle size distribution of water-soluble CdTe quantum dots by optical spectroscopy, RSC Adv. 4 (2014) 36024–36030.

[43] X. Gao, Y. Lu, M. Liu, S. He, W. Chen, Sub-nanometer sized Cu6(GSH)3 clusters: one-step synthesis and electrochemical detection of glucose, J. Mater. Chem. C 3 (2015) 4050–4056.

[44] X. Chen, Z. Guo, P. Miao, One-pot synthesis of GSH-Capped CdTe quantum dots with excellent biocompatibility for direct cell imaging, Heliyon 4 (2018) e00576, e00576.

[45] J.K. Cooper, A.M. Franco, S. Gul, C. Corrado, J.Z. Zhang, Characterization of primary amine capped CdSe, ZnSe, and ZnS quantum dots by FT-IR: determination of surface bonding interaction and identification of selective desorption, Langmuir: the ACS journal of surfaces and colloids 27 (2011) 8486–8493.
[46] S. Huang, H. Qiu, Q. Xiao, C. Huang, W. Su, B. Hu, A simple QD-FRET bioprobe for sensitive and specific detection of hepatitis B virus DNA, J. Fluoresc. 23 (2013) 1089–1098.
[47] W.J. Parak, D. Gerion, D. Zanchet, A.S. Woerz, T. Pellegrino, C. Micheel, S.C. Williams, M. Seitz, R.E. Bruehl, Z. Bryant, C. Bustamante, C.R. Bertozzi, A.P. Alivisatos, Conjugation of DNA to silanized colloidal semiconductor nanocrystalline quantum dots, Chem. Mater. 14 (2002) 2113–2119.
[48] G. Pereira, C. Monteiro, G. Albuquerque, M. Pereira, M. Cabrera, P. Filho, G. Pereira, A. Fontes, B. Santos, (Bio)conjugation strategies applied to fluorescent semiconductor quantum dots, J. Braz. Chem. Soc. 30 (2019).
[49] S. Kumar Panigrahi, A. Kumar Mishra, Inner filter effect in fluorescence spectroscopy: as a problem and as a solution, J. Photochem. 41 (2019), 100318.
[50] J.J. Beato-López, M.L. Espinazo, C. Fernández-Ponce, E. Blanco, M. Ramírez-del-Solar, M. Domínguez, F. García-Cózar, R. Litrán, CdTe quantum dots linked to Glutathione as a bridge for protein crosslinking, J. Lumin. 187 (2017) 193–200.
[51] M. Grabolle, M. Spieles, V. Lesnyak, N. Gaponik, A. Eychmüller, U. Resch-Genger, Determination of the fluorescence quantum yield of quantum dots: suitable procedures and achievable uncertainties, Anal. Chem. 81 (2009) 6285–6294.
[52] Y. Zheng, S. Gao, J. Ying, Synthesis and cell-imaging applications of glutathione-capped CdTe quantum dots, Adv. Mater. 19 (2007) 376–380.
[53] S. Melle, O.G. Calderón, M. Laurenti, D. Mendez-Gonzalez, A. Egatz-Gómez, E. López-Cabarcos, E. Cabrera-Granado, E. Díaz, J. Rubio-Retama, Förster resonance energy transfer distance dependence from upconverting nanoparticles to quantum dots, J. Phys. Chem. C 122 (2018) 18751–18758.
[54] A. Samanta, S. Buckhout-White, E. Oh, K. Susumu, I.L. Medintz, Exploring attachment chemistry with FRET in hybrid quantum dot dye-labeled DNA dendrimer composites, Mol. Syst. Des. Eng. 3 (2018) 314–327.
[55] G.R. Bardajee, M. Zamani, H. Mahmoodian, H. Elmizadeh, H. Yari, L. Jouyandeh, R. Shirkavand, M. Sharifi, Capability of novel fluorescence DNA-conjugated CdTe/ZnS quantum dots nanoprobe for COVID-19 sensing, Spectrochim. Acta Mol. Biomol. Spectrosc. 269 (2022), 120702.
[56] H. Elmizadeh, M. Soleimani, F. Faridbod, G.R. Bardajee, A sensitive nano-sensor based on synthetic ligand-coated CdTe quantum dots for rapid detection of Cr(III) ions in water and wastewater samples, Colloid Polym. Sci. 296 (2018) 1581–1590.